Journal of Computational Physics 288 (2015) 52–65

Contents lists available at ScienceDirect

Journal of Computational Physics

www.elsevier.com/locate/jcp

A comparative study of an asymptotic preserving scheme and unified gas-kinetic scheme in continuum flow limit

Songze Chen, Kun Xu *

Hong Kong University of Science and Technology, Clear Water Bay, Kowloon, Hong Kong, China

ARTICLE INFO

Article history:
Received 19 July 2013
Received in revised form 5 August 2014
Accepted 14 February 2015
Available online 19 February 2015

Keywords:
Asymptotic preserving schemes
Unified gas kinetic schemes

ABSTRACT

Asymptotic preserving (AP) schemes target to simulate both continuum and rarefied flows. Many existing AP schemes are capable of recovering the Euler limit in the continuum regime. However, to get accurate Navier–Stokes solutions is still challenging. In order to distinguish physical mechanism underlining different AP schemes, an implicit–explicit (IMEX) AP method and the unified gas kinetic scheme (UGKS) are employed to solve the Bhatnagar–Gross–Krook (BGK) kinetic equation in both transition and continuum flow regimes. As a benchmark test case, the lid-driven cavity flow is used for evaluating numerical performance of these two AP schemes. The numerical results show that the UGKS captures the viscous solution accurately. The velocity profiles converge to the classical benchmark solutions in continuum regime with the mesh size being much larger than the local particle mean free path. However, the IMEX AP scheme seems to have difficulty to get these solutions in the corresponding limit. The analysis demonstrates that the dissipation of AP schemes has to be properly controlled in the continuum flow regime through a delicate numerical treatment of collision and convection of the kinetic equation. Physically, it becomes necessary to couple both the convection and collision terms in the flux evaluation in order to recover correct Navier–Stokes limit.

1. Introduction

The description of a gas flow depends on the resolution to identify the flow physics. On the macroscopic level of hydrodynamic scale, the well-defined governing equations for fluid system are the Euler equations and Navier–Stokes (NS) equations. On the other hand, if the resolution goes to particle mean free path scale, the Boltzmann equation can be used to describe a microscopic flow system. In early 20th century, Chapman and Enskog [1] independently deduced the Navier–Stokes equations from the Boltzmann equation under certain scale stretching approximation. Specifically, when the Knudsen number (Kn), which is defined as the ratio between the mean free path (λ) and the characteristic length of the problem, is small, say, $\mathrm{Kn} \ll 1$, the viscosity and heat conduction coefficients in the Navier–Stokes equations are quantitatively evaluated according to the intermolecular forces. Their work bridges flow descriptions on different scales. However, for a numerical solver, it is difficult to achieve such an asymptotic limit. In continuum flow regime, an explicit numerical solver for kinetic equations provides too much detailed information which is not needed and the scheme suffers from small time step and cell size due to its kinetic scale resolution. Therefore, many studies have been focused on the development of a unified numerical scheme. There are many possible approaches, such as domain decomposition strategies and hybrid methods, etc.

* Corresponding author.
E-mail addresses: jacksongze@gmail.com (S. Chen), makxu@ust.hk (K. Xu).

http://dx.doi.org/10.1016/j.jcp.2015.02.014
0021-9991/

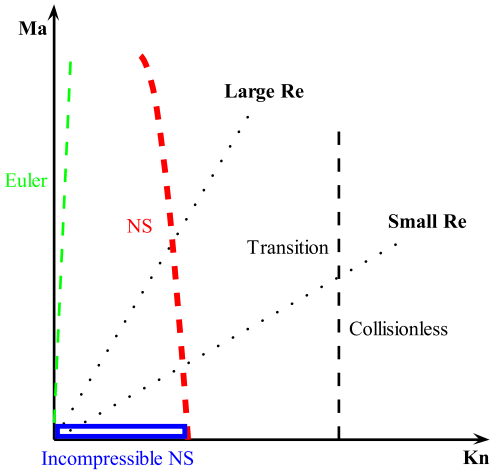

Fig. 1. A sketch for different flow regimes on Kn–Ma plane. The dotted lines represent isolines of Reynolds number.

[2–4]. This paper is mainly concerned with the unified kinetic scheme which is applicable for the flow description in the whole flow regimes.

A numerical scheme, which is capable of capturing the characteristic behavior on different scales with a fixed discretization in both space and time, is called asymptotic preserving scheme [5]. Specifically, for a gas system, it requires the AP scheme to recover the NS limit and Euler limit on fixed time step and mesh size as the Knudsen number goes to zero. A standard explicit scheme for kinetic equation always requires the space and time discretizations to resolve the kinetic scale of the system, such as the particle mean free path. It makes the scheme tremendously expensive when the system is close to the continuum limit. In recent years, many studies have been concentrated on the development of AP schemes. It has been shown that delicate time [6,7] and space [8] discretizations should be adopted in order to achieve AP property. Physically, the continuum limit is associated with intensive particle collisions. The local velocity distribution function rapidly approaches to a local equilibrium state. Based on this fact, it is clear that any plausible approximation to the collision process must project the non-equilibrium state to the local equilibrium one. Previous results [6,7,9] show that an effective condition for the numerical scheme to recover the correct continuum limit is to project the distribution function to the local equilibrium one with a discrete analogue of the asymptotic expansion of the continuous equations. In these studies, implicit time discretization is implemented to meet requirement of numerical stability and AP property. On the other hand, it seems that the space discretization is not as crucial as the time discretization in the sense of AP property. However, the sophisticated space discretization is still necessary for the capturing of correct long-time behavior of hyperbolic systems with stiff relaxation terms [8]. The asymptotic balance must be taken into account in the space discretization. Similar principle for space discretization has been proposed in the gas kinetic scheme (GKS) [10,11]. The essential ingredient of GKS is the implementation of a local analytical solution which allows the collision effect to participate in construction of the space discretization of the equilibrium state. Unified gas kinetic scheme [12] solves the gas distribution function directly. And it also employs the local analytical solution which allows UGKS to recover continuum limit asymptotically.

Although all AP schemes are able to obtain the Euler limit, only a few studies are targeting to the AP property of recovering NS solutions [12–15]. The operator splitting strategy of decoupling transport and collision always results in the Euler AP property [13]. Any excessive dissipation in the AP schemes can be considered as an artificial dissipation in the Euler limit, as long as it is consistent with the numerical scheme of the Euler equations. The Navier–Stokes limit is characterized by the dissipation which is well-defined. For the Navier–Stokes limit, the numerical dissipation has to be controlled and be less than the physical one. A Navier–Stokes AP property can be obtained by including the convection terms in the collision process [13–15]. But this kind of schemes may involve excessive artificial dissipation from the numerical treatment of spatial derivatives. As a result, the time accuracy can only have first order. Bennoune et al. constructed a NS AP scheme using equilibrium and non-equilibrium splitting technique. Their analysis shows that the dissipative term is identical to the Chapman–Enskog expansion [13]. However, they ignored the large numerical dissipation in the Euler flux which is evaluated by solving the collisionless Boltzmann equation.

In the past years, many AP schemes and unified gas-kinetic scheme have been developed. The implicit scheme with the implementation of the convection term into the collision process is accepted as a strategy for the Euler AP property. But the AP property for the Navier–Stokes limit has not been extensively validated. Moreover, a practical and useful multiscale computation is to get a correct transition from kinetic solution to the Navier–Stokes limit, rather than the Euler limit. Fig. 1 shows the flow regimes on Kn–Ma plane. The vertical axis represents the Euler limit, and the horizontal axis from origin to the transition regime represents the incompressible NS limit. This figure clearly shows that, when the Knudsen number decreases, the asymptotic behavior of a gas system results in NS limit first, then Euler limit. In another direction, as Mach number decreases, the incompressible NS limit emerges and is followed by the Stokes flow limit with the further decreasing

of the Mach number. There is no path to achieve Euler limit by circumventing NS limit. Therefore, the NS AP property is important for any AP scheme to describe the asymptotic behavior. And it is of great engineering application value. In this study, we only consider the asymptotic process to (weakly) compressible NS limit. As shown in the figure, as long as the Mach number is large enough, the flow system can be regarded as compressible flow. For the incompressible NS and Stokes flow limit, please refer to [16].

The main purpose of this paper is to set up a benchmark test case for validating the NS limit for any AP scheme. The Bhatnagar–Gross–Krook (BGK) model is adopted for the development of AP schemes because it is the simplest kinetic model equation. We are going to compare the numerical results of these AP schemes in the lid-driven cavity flow simulations with the well-defined reference data [17]. Then, the principle to recover the NS AP limit will be presented. The remaining parts of this paper are organized as follows. Section 2 introduces the AP schemes. Section 3 shows the numerical results. Section 4 discusses the dissipative mechanism and the relation to the treatment of particle collision and convection. Section 5 gives the conclusion.

2. AP schemes

2.1. Bhatnagar–Gross–Krook model

The Bhatnagar–Gross–Krook model was proposed to simplify the Boltzmann equation [18]. It takes the following form,

$$\frac{\partial f}{\partial t}+\mathbf{u}\cdot\frac{\partial f}{\partial \mathbf{x}}=\frac{g-f}{\tau}, \tag{1}$$

where $f(\mathbf{x},\mathbf{u},t)$ represents the particle velocity distribution function. It is a function of location $\mathbf{x}$, particle velocity $\mathbf{u}$, and time t. Here τ denotes the relaxation time. The conservative variables W can be obtained by taking moments of f,

$$W=\begin{pmatrix}\rho\\ \rho\mathbf{U}\\ \rho E\end{pmatrix}=\int \psi f d\mathbf{u} = < f >,$$

where $\psi=(1,\mathbf{u},\frac{1}{2}\mathbf{u}^2)^T$. In this study, we only consider monatomic gas, thus ignore the internal degree of freedom. The right hand side of Eq. (1) represents the relaxation process. Here g is the equilibrium state which reads,

$$g=\mathcal{M}(f)=\rho\left(\frac{1}{2\pi RT}\right)^{\frac{3}{2}}e^{-\frac{1}{2RT}(\mathbf{u}-\mathbf{U})^2}, \tag{2}$$

where $\mathcal{M}(f)$ returns a Maxwell distribution function with identical conservative moments of f, namely, $< g > = < f >$. Here T denotes temperature and R is gas constant. It is a standard procedure to get the Navier–Stokes equations via the Chapman–Enskog expansion of the BGK model. In continuum flow regime, the particle distribution function f can be expanded in a power series of the small parameter τ when $\tau\to 0$. For simplicity, only the first two terms are considered here,

$$f=f^{(0)}+\tau f^{(1)}+O(\tau^2). \tag{3}$$

All deviations from the equilibrium state preserve zero moments for the conservative variables, namely,

$$\int \psi f^{(1)} d\mathbf{u}=0. \tag{4}$$

Substitute Eq. (3) into the BGK model,

$$f_t^{(0)}+\tau f_t^{(1)}+\mathbf{u}\cdot\nabla f^{(0)}+\tau\mathbf{u}\cdot\nabla f^{(1)}+O(\tau^2)=\frac{g-f^{(0)}}{\tau}-f^{(1)}+O(\tau). \tag{5}$$

The first order Chapman–Enskog equation for $f^{(0)}$ is obtained by equating terms of $O(\frac{1}{\tau})$, that is

$$g-f^{(0)}=0.$$

Up to this order, $f=f^{(0)}=g$. Substituting this formula into the BGK model and then taking the conservative moments, we get the Euler equations.

$$< f_t^{(0)}+\mathbf{u}\cdot\nabla f^{(0)} > = < \frac{g-f}{\tau} > \Rightarrow$$
$$\begin{pmatrix}\rho\\ \rho\mathbf{U}\\ \rho E\end{pmatrix}_t+\nabla\cdot\begin{pmatrix}\rho\mathbf{U}\\ \rho\mathbf{U}\mathbf{U}+p\mathbf{I}\\ (\rho E+p)\mathbf{U}\end{pmatrix}=0, \tag{6}$$

where $\mathbf{I}$ denotes identity matrix, and p is pressure. The equation corresponding on the order $O(\tau^0)$ is

$$f_t^{(0)} + \mathbf{u}\cdot\nabla f^{(0)} = -f^{(1)}.$$

From the above equation we get,

$$f^{(1)} = -(g_t + \mathbf{u}\cdot\nabla g). \tag{7}$$

Now the expansion (3) turns out to be,

$$f = g - \tau(g_t + \mathbf{u}\cdot\nabla g) + O(\tau^2). \tag{8}$$

Substituting the formula (8) into the BGK equation, and neglecting higher order terms, we have

$$(f_t^{(0)} + \mathbf{u}\cdot\nabla f^{(0)}) + \tau(f_t^{(1)} + \mathbf{u}\cdot\nabla f^{(1)}) = \frac{g-f}{\tau}. \tag{9}$$

Taking conservative moments on the above equation gives the Navier–Stokes equations. Specifically, the conservative moments of the right hand side are zero. The first part of the left hand side is identical to the Euler equations. Only the second term on the left hand side is related to the shear stress and the heat flux which characterize the Navier–Stokes equations. The moments of the forepart, $\int \psi\tau f_t^{(1)} d\mathbf{u}$, is 0 due to the expansion constraint (Eq. (4)). By substituting the formula (7) into Eq. (9), the remaining part of the conservative moments represents the dissipation terms.

$$\begin{pmatrix}\rho\\ \rho\mathbf{U}\\ \rho E\end{pmatrix}_t + \nabla\cdot\begin{pmatrix}\rho\mathbf{U}\\ \rho\mathbf{U}\mathbf{U}+p\mathbf{I}\\ (\rho E+p)\mathbf{U}\end{pmatrix} - \tau\nabla\cdot <\mathbf{u}(g_t+\mathbf{u}\cdot\nabla g)> = 0. \tag{10}$$

Here g_t and ∇g are evaluated by differentiating Eq. (2),

$$g_t = g[\frac{\rho_t}{\rho} - \frac{3T_t}{T} + \frac{(\mathbf{u}-\mathbf{U})^2 T_t}{2RT^2} + \frac{(\mathbf{u}-\mathbf{U})\cdot\mathbf{U}_t}{RT}],$$
$$\nabla g = g[\frac{\nabla\rho}{\rho} - \frac{3\nabla T}{T} + \frac{(\mathbf{u}-\mathbf{U})^2\nabla T}{2RT^2} + \frac{(\mathbf{u}-\mathbf{U})\cdot\nabla\mathbf{U}}{RT}].$$

Then the time derivatives in g_t are replaced by space derivatives using the Euler equations. And we get,

$$g_t + \mathbf{u}\cdot\nabla g = g[\frac{\mathbf{u}-\mathbf{U}}{T}\cdot\nabla T(\frac{(\mathbf{u}-\mathbf{U})^2}{2RT} - \frac{5}{2}) + \frac{1}{RT}(\mathbf{u}-\mathbf{U})\cdot(\nabla\mathbf{U})\cdot(\mathbf{u}-\mathbf{U}) - \frac{(\mathbf{u}-\mathbf{U})^2}{3RT}\nabla\cdot\mathbf{U}].$$

Therefore,

$$\begin{aligned} -\tau\nabla\cdot <\mathbf{u}(g_t+\mathbf{u}\cdot\nabla g)> &= \nabla\cdot\begin{pmatrix}0\\ \mathbf{p}\\ (\mathbf{q}+\mathbf{p}\cdot\mathbf{U})\end{pmatrix}\\ &= \nabla\cdot\begin{pmatrix}0\\ -\mu((\nabla\mathbf{U}+(\nabla\mathbf{U})^T) - \frac{2}{3}(\nabla\cdot\mathbf{U})\mathbf{I}))\\ -\kappa\nabla T + \mathbf{p}\cdot\mathbf{U}\end{pmatrix} \end{aligned} \tag{11}$$

where $\mu = \tau p$ and $\kappa = \frac{5R}{2}\mu$.

As shown by the above derivation, the deviation from the equilibrium state, namely, $-\tau(g_t + \mathbf{u}\cdot\nabla g)$, dominates the asymptotic process and gives the Navier–Stokes limit. We take the formula (8) as a rule to measure the dissipation of numerical schemes in the NS limit.

2.2. Implicit–explicit discretization for collision term

Owing to the stiffness of the BGK relaxation model, the standard explicit scheme requests very small time step. To overcome this difficulty, implicit scheme for collision term has to be adopted when the Knudsen number approaches to 0. Thanks to the conservation laws, the implicit term can be solved explicitly. Here, we introduce a simple implicit–explicit scheme as illustration [15,19],

$$\frac{f_i^{n+1} - f_i^n}{\Delta t} + \mathbf{u}\cdot\nabla f_i^n = \frac{g_i^{n+1} - f_i^{n+1}}{\tau_i^{n+1}}. \tag{12}$$

The convection term will be discretized later. Taking conservative moments of this equation, we have,

$$\frac{W_i^{n+1} - W_i^n}{\Delta t} + <\mathbf{u}\cdot\nabla f_i^n> = 0. \tag{13}$$

Here, $< \mathbf{u}\cdot\nabla f_i^n >$ denotes the corresponding macroscopic fluxes which will be introduced later. So the conservative variables W_i^{n+1} can be obtained explicitly. Then, g_i^{n+1} and τ_i^{n+1} are fully determined because there is one to one correspondence between macroscopic variables and the equilibrium state. Therefore, we have

$$f_i^{n+1} = \frac{\tau_i^{n+1}}{\tau_i^{n+1}+\Delta t}[f_i^n - \Delta t\mathbf{u}\cdot\nabla f_i^n] + \frac{\Delta t}{\tau_i^{n+1}+\Delta t}g_i^{n+1}. \tag{14}$$

Assuming $f_i^n = g_i^n + O(\tau)$, then reformulate f_i^{n+1} as follows,

$$f_i^{n+1} = g_i^{n+1} - \tau_i^{n+1}[\frac{f_i^{n+1}-f_i^n}{\Delta t} + \mathbf{u}\cdot\nabla f_i^n]. \tag{15}$$

Therefore, $f_i^{n+1} = g_i^{n+1} + O(\tau)$ is also satisfied. Then substituting it into above formula, f_i^{n+1} reads,

$$f_i^{n+1} = g_i^{n+1} - \tau_i^{n+1}[\frac{g_i^{n+1}-g_i^n}{\Delta t} + \mathbf{u}\cdot\nabla g_i^n] + O(\tau^2). \tag{16}$$

For single step schemes, the spacial derivative, ∇g_i^n, involved in the Chapman–Enskog expansion is generated from the previous time step. It gives the following estimation,

$$f_i^{n+1} = g_i^{n+1} - \tau^{n+1}[(g_i^{n+1})_t + \mathbf{u}\cdot\nabla g_i^{n+1}] + O(\tau\Delta t) + O(\tau^2). \tag{17}$$

Comparing it with Eq. (8), there is an additional dissipation of order $O(\tau\Delta t)$ at $n+1$ time step. It is a good estimation for the Navier–Stokes AP limit, since non-dimensional time step is always smaller than 1, namely, $\Delta t << 1$. However, a distribution function close to the Chapman–Enskog expansion is only a good starting point. It cannot lead to NS AP property automatically if the numerical flux cannot be properly evaluated. For example, the first order kinetic flux vector splitting (KFVS) method uses exact equilibrium state as initial condition in each cell, but the scheme is quite dissipative. As we know, the dissipation in NS equations is a macroscopic conception, and it is determined by the moments of a distribution function. Only through the flux term, such as Eq. (11), a distribution function can effect the dissipation of the scheme. Therefore, it is insufficient to get insight of the dissipation by merely making comparison between f^{n+1} and the Chapman–Enskog expansion. The error introduced in the numerical evaluation of fluxes determines the quality of the scheme. In order to understand and estimate the real dissipation in AP scheme, we must investigate the discretization of the convection term, such as $\mathbf{u}\cdot\nabla f_i^n$ in Eq. (14).

2.3. Discretization of convection terms

Taking one dimensional case as an example, the discrete convection term is written in a conservative form,

$$(uf_i^n)_x = \frac{F_{i+1/2}-F_{i-1/2}}{\Delta x}. \tag{18}$$

where F denotes numerical flux at cell interface.

2.3.1. IMEX AP scheme

The numerical flux for IMEX AP scheme at $x_{i+1/2}$ is given below,

$$\mathcal{F}_{IMEX} = uf_{i+1/2}. \tag{19}$$

The cell interface distribution function is defined as,

$$\begin{aligned} f_{i+1/2}^l &= f_i + \frac{\Delta x}{2}S^l, \\ f_{i+1/2}^r &= f_{i+1} - \frac{\Delta x}{2}S^r, \\ f_{i+1/2} &= H(u)f_{i+1/2}^l + (1-H(u))f_{i+1/2}^r, \end{aligned} \tag{20}$$

where $H(u)$ is Heaviside function,

$$H(u) = \begin{cases} 0, & u<0, \\ 1, & u\geq 0, \end{cases} \tag{21}$$

and S^l, S^r represent slopes with a slope limiter. In this study, the van Leer slope limiter is used.

2.3.2. Unified gas kinetic scheme

The key ingredient of the unified gas kinetic scheme is to couple the collision effect into the convection term. The earliest application of this idea is the gas kinetic scheme (GKS) for the Navier–Stokes solutions [10,11]. The unified gas kinetic scheme (UGKS) makes a major step forward [12,20–22]. It solves the kinetic equation in all flow regimes including the free molecular and the Navier–Stokes limits. The main difference between the UGKS and the IMEX AP scheme is the discretization of convection terms.

The numerical flux of UGKS is derived by considering the local analytical solution,

$$\mathcal{F}_{UGKS} = \frac{1}{\Delta t}\int_0^{\Delta t} uf(t)dt.$$

The local analytical solution is given below,

$$\begin{aligned} f(x,u,t) &= e^{-t/\tau} f_0(x-ut) \\ &\quad + \frac{1}{\tau}\int_0^t g(x',u,t')e^{-(t-t')/\tau}dt', \end{aligned} \tag{22}$$

where $x' = x - u(t-t')$. Here f_0 is almost the same as $f_{i+1/2}$ in IMEX AP scheme, but it is only taken as the initial condition at the beginning of each time step. Suppose the cell interface is located at the origin ($x = 0$), the initial gas distribution function is,

$$\begin{aligned} f_0(x) &= H(u)(f_i + (x + \frac{\Delta x}{2})S^l) + (1 - H(u))(f_{i+1} + (x - \frac{\Delta x}{2})S^r) \\ &= f_{i+1/2} + H(u)xS^l + (1 - H(u))xS^r. \end{aligned} \tag{23}$$

The inclusion of the equilibrium part, $g(x,t,u)$, is the key of UGKS. It is formally written as,

$$g(x,t,u) = g_{i+1/2}(1 + ax + At), \tag{24}$$

where $g_{i+1/2} = \mathcal{M}(f_{i+1/2})$. In the Taylor expansion of an equilibrium state, a and A [11] represent the spatial and temporal derivatives of the equilibrium state respectively. Then the interface flux of UGKS is written as,

$$\begin{aligned} \Delta t\mathcal{F}_{UGKS} &= \int_0^{\Delta t} uf(t)dt \\ &= u\{\tau(1 - e^{-\Delta t/\tau})\,(H(u)f^l_{i+1/2} + (1 - H(u))f^r_{i+1/2}) \\ &\quad + \tau(\tau(e^{-\Delta t/\tau} - 1) + \Delta t e^{-\Delta t/\tau})\,u(H(u)S^l + (1 - H(u))S^r) \\ &\quad + (\Delta t - \tau(1 - e^{-\Delta t/\tau}))\,g_{i+1/2} \\ &\quad + \tau(2\tau(1 - e^{-\Delta t/\tau}) - \Delta t(1 + e^{-\Delta t/\tau}))\,aug_{i+1/2} \\ &\quad + (\frac{1}{2}(\Delta t)^2 + \tau(\tau(1 - e^{-\Delta t/\tau}) - \Delta t))\,Ag_{i+1/2}\}. \end{aligned} \tag{25}$$

Although this expression seems very complicated, it could be written in a concise form with clear physical meaning. This will be discussed later.

2.4. Boundary condition

Boundary condition is a crucial part of a numerical scheme. We need a unified solid boundary condition to complete AP scheme. Before proposing such a boundary condition, we introduce the kinetic fully diffusion boundary condition (KBC) at first. Suppose normal direction $\mathbf{n}$ towards the solid is the positive direction. The incoming distribution function at boundary is represented by f_{gas}, which is interpolated from inner cells. The distribution function of the particles emitted from the solid wall is a Maxwell distribution function,

$$g_W = \rho_W\left(\frac{1}{2\pi RT_W}\right)^{\frac{3}{2}} e^{-\frac{1}{2RT_W}((\mathbf{u}-\mathbf{U}_W)^2)},$$

where T_W and $\mathbf{U}_W$ are given by solid boundary. Then no penetration condition is used to determine ρ_W, i.e.,

$$\int_{\mathbf{n}\cdot(\mathbf{u}-\mathbf{U}_W)\geq 0} \mathbf{n}\cdot(\mathbf{u}-\mathbf{U}_W)f_{gas}d\mathbf{u} = \int_{\mathbf{n}\cdot(\mathbf{u}-\mathbf{U}_W)<0} \mathbf{n}\cdot(\mathbf{u}-\mathbf{U}_W)g_W d\mathbf{u}. \tag{26}$$

The above Maxwell boundary condition works very well in the rarefied flow regime, but it may not work properly in the continuum flow limit. In the above Maxwell boundary construction, the Knudsen layer will be enlarged since it assumes that the particles coming from gas collide with the solid boundary directly without suffering from any inter-molecule collisions. Moreover, the extrapolation will violate the non-slip boundary condition in continuum flow unless the cell side is sufficiently small to resolve the Knudsen layer. If we change the Maxwell boundary condition to a simple bounce back boundary condition for the non-slip boundary condition, it cannot work properly for the rarefied gas flow where velocity slip appears. Therefore, in order to get a valid boundary condition for both rarefied and continuum flows, a multiscale boundary condition (MBC) is required for all Knudsen number regime.

Here, we propose a multiscale boundary condition. The idea is to use local solution again, namely, f_{gas} is replaced by $f(t)$ defined by formula (22).

$$\int_0^{\Delta t}\int_{\mathbf{n}\cdot(\mathbf{u}-\mathbf{U}_W)\geq 0}\mathbf{n}\cdot(\mathbf{u}-\mathbf{U}_W)f(t)d\mathbf{u}dt=\int_0^{\Delta t}\int_{\mathbf{n}\cdot(\mathbf{u}-\mathbf{U}_W)<0}\mathbf{n}\cdot(\mathbf{u}-\mathbf{U}_W)g_W d\mathbf{u}dt. \tag{27}$$

Similar boundary condition has been developed for the radiative transfer problem [23]. The gas initial spatial distribution f_0 is also reconstructed by extrapolation from inner cells. The local equilibrium state $g_{i+1/2}$ is determined from the no slip boundary condition, say,

$$T_{i+1/2}=T_W,$$
$$\mathbf{U}_{i+1/2}=\mathbf{U}_W.$$

The pressure of $g_{i+1/2}$ is set to the same pressure at the adjacent cell center. Then, the density of $g_{i+1/2}$ is fully determined,

$$\rho_{i+1/2}=\rho_{gas}T_{gas}/T_W.$$

This boundary condition only changes the incoming distribution function. The particles emitted from the boundary also obey the fully diffusion assumption. In the following section, both the original Maxwell kinetic boundary condition (KBC) and the current multiscale boundary condition (MBC) are implemented in the numerical schemes.

3. Numerical experiments

The Navier–Stokes limit is characterized by shear flow. This kind of flow feature does not appear in one dimensional case. Thus, we choose lid-driven cavity flow as a benchmark. A transition cavity flow is solved to make sure the performance of two AP schemes for capturing rarefied flow behavior. The working gas is argon with temperature viscosity relation $\mu\sim T^{\omega}$, where $\omega=0.81$. The reference viscosity is defined as [24]

$$\mu_{ref}=\frac{15}{(7-2\omega)(5-2\omega)}\frac{\rho\lambda\sqrt{2\pi RT}}{2}, \tag{28}$$

where λ is the mean free path. We choose $\mathrm{Kn}=0.1$ ($\mathrm{Re}=1.9345$) for the first case. The Mach number is about 0.15. The top wall moves from left to right. The computational domain is $[0,1]\times[0,1]$ which is covered by 61×61 uniform mesh points in the physical space. The discretization in velocity space is 40×40. The ratio between the time step and the relaxation time, $\Delta t/\tau$, is about 0.014. Fig. 2 shows the flow field from two schemes. They are almost identical. The velocity profiles (Fig. 3) from both schemes are indistinguishable along the vertical central line and the horizontal central line. Therefore, it is confirmed that both UGKS and IMEX AP scheme obtain the same result in transition flow regime. Both KBC and MBC are tested, and they perform equally well.

Then, we reduce the Knudsen number until the Reynolds number is equal to 1000. Correspondingly, $\Delta t/\tau$ increases to about 7.2. The mesh in physical space keeps 61×61, and the mesh in velocity space is 20×20. Note that, the mesh points in the velocity space can be reduced due to the regular distribution function in continuum flow regime. The cavity flow at $\mathrm{Re}=1000$ is a typical continuum flow regime. The Mach number is 0.15. The numerical results are compared with classical benchmark solutions from Ghia [17]. Fig. 4 shows the stream lines in the cavity. The boundary condition is MBC for UGKS, and KBC for IMEX AP scheme. Compared with the solution in transition regime, the eddies emerge at the bottom corners. The vortex from UGKS is obviously more intensive than that from IMEX AP scheme. The velocity profiles along the central line shown in Fig. 5 demonstrate that the accuracy of UGKS is better than that of IMEX AP in NS limit.

The boundary condition could strongly affect the final results. Therefore, in order to have a complete understanding of boundary condition effect, we design another two combinations of schemes and boundary conditions, namely, UGKS+KBC and IMEX+MBC. The MBC in the IMEX AP scheme uses UGKS to calculate the flux at boundary, since IMEX AP doesn't have equilibrium part in the numerical flux. As shown in Fig. 6, both results seem more dissipative than UGKS+MBC. The eddies in the corners are also smaller. This is because that the KBC enlarges the Knudsen layer which should be much thinner than the cell size in the continuum flow. And the enlarged Knudsen layer smears the eddies near the boundary. This phenomenon is more obvious on coarse mesh as shown in Fig. 7. On the other hand, the IMEX+MBC doesn't change too much in comparison with IMEX+KBC. It seems that the IMEX AP solver could not recover the hydrodynamic NS solution even with MBC. According to the simulation results, the UGKS+MBC is the best scheme among four combinations (Figs. 4 to 8).

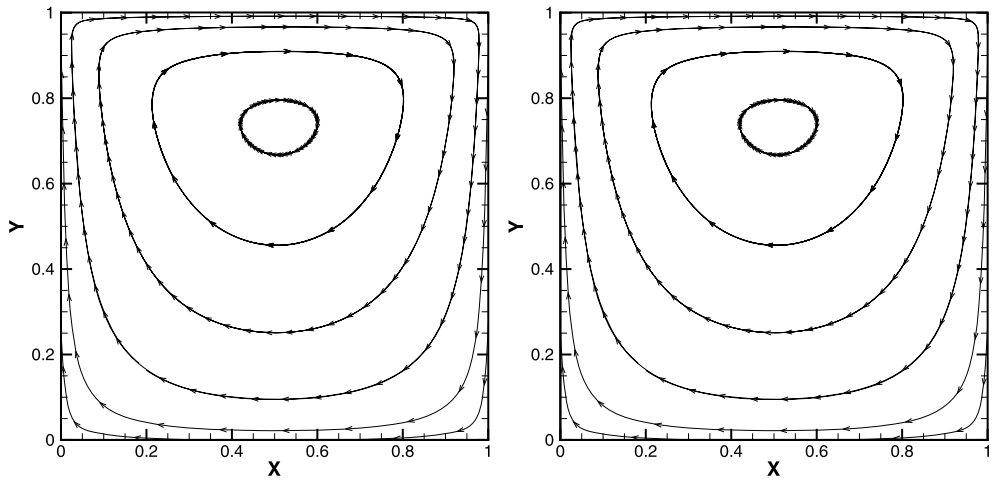

Fig. 2. The stream lines for lid-driven cavity flow at Kn = 0.1 with 61×61 mesh points in the physical space and 40×40 mesh points in the velocity space. The left is from IMEX AP scheme and the right is from UGKS.

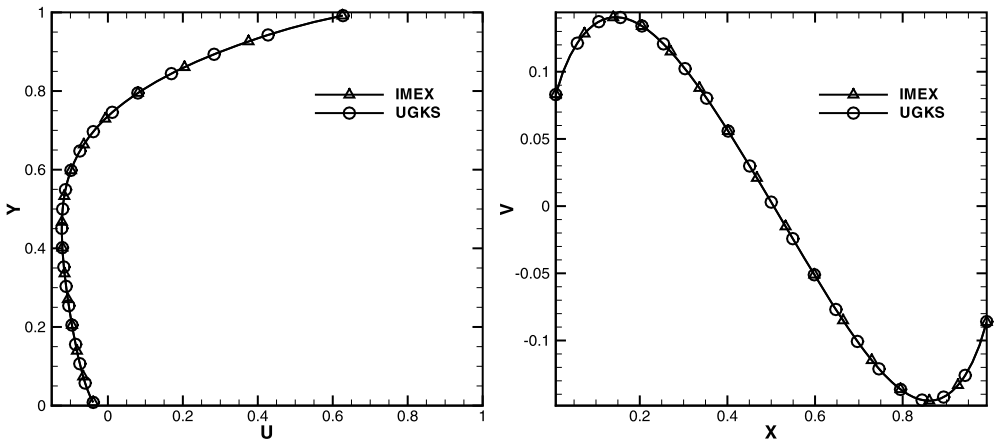

Fig. 3. The velocity profiles along the vertical and horizontal central lines at Kn = 0.1.

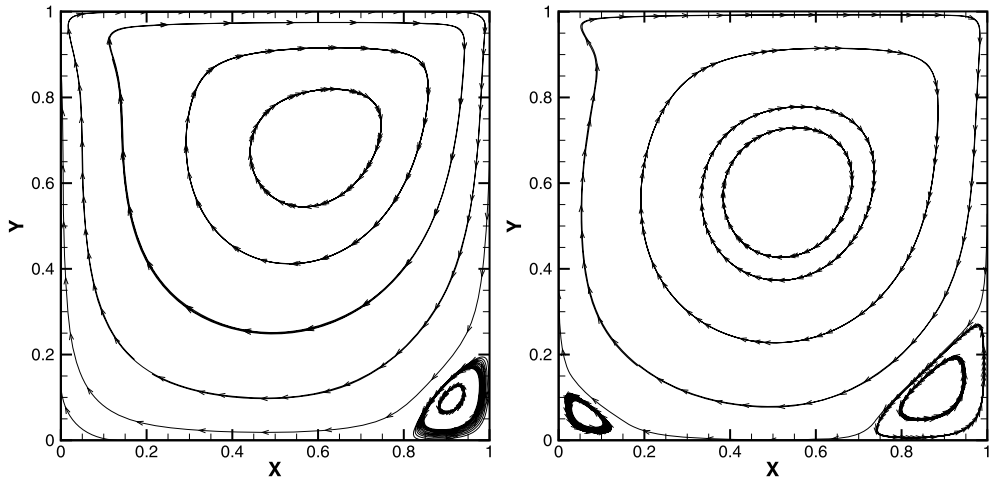

Fig. 4. The stream lines for lid-driven cavity flow at Re = 1000. The left is from IMEX AP scheme, and right is from UGKS.

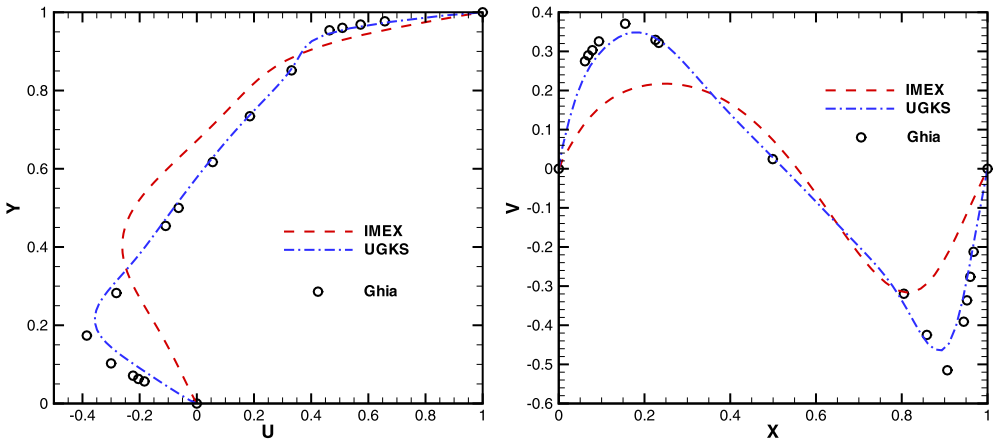

Fig. 5. The velocity profiles along the vertical and horizontal central lines at Re = 1000.

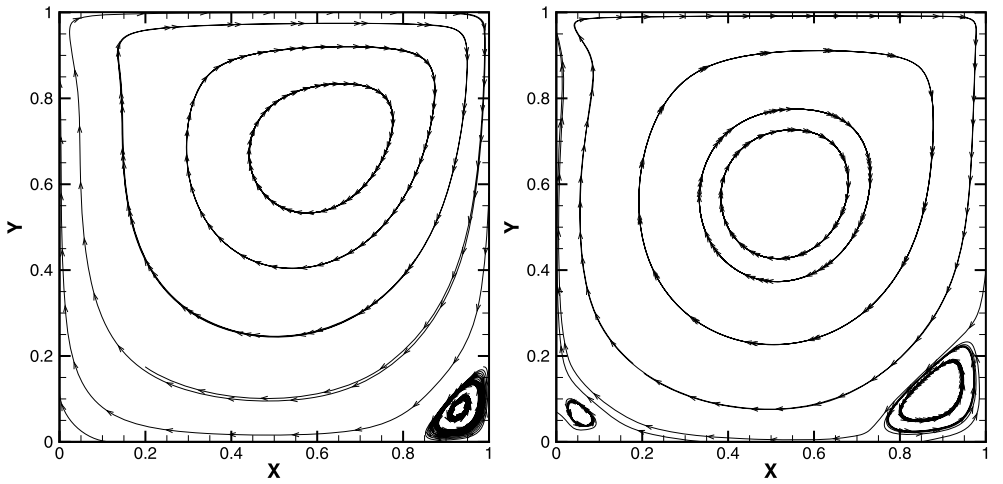

Fig. 6. The stream lines derived by AP schemes with different boundary conditions at Re = 1000. The left is IMEX+MBC, and the right is UGKS+KBC.

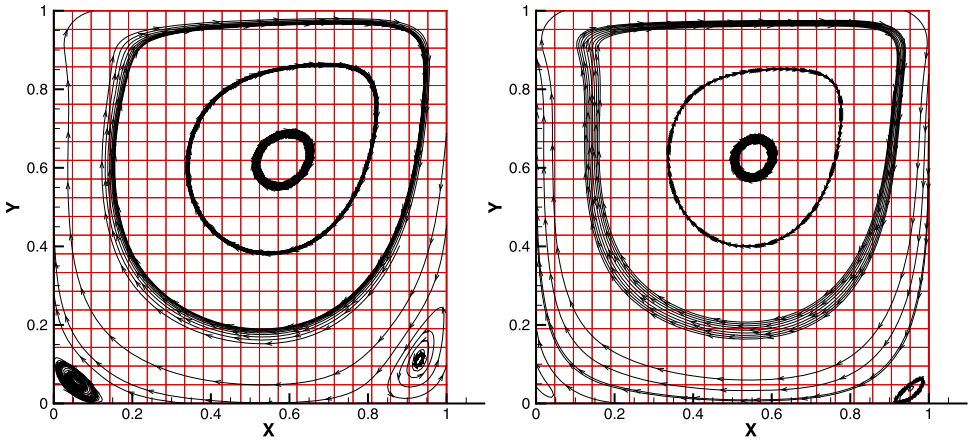

Fig. 7. The stream lines on coarse mesh (21×21) derived by UGKS with MBC (left) and KBC (right) at Re = 1000.

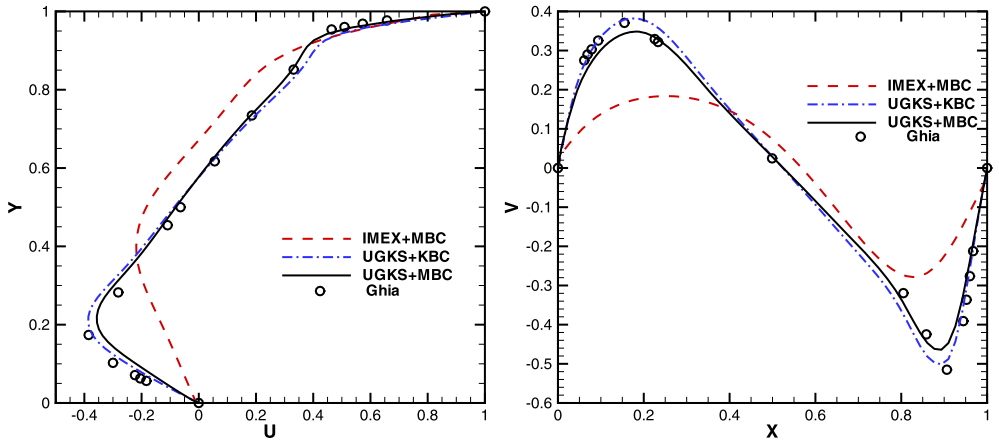

Fig. 8. The comparison of IMEX AP and UGKS using the different boundary conditions.

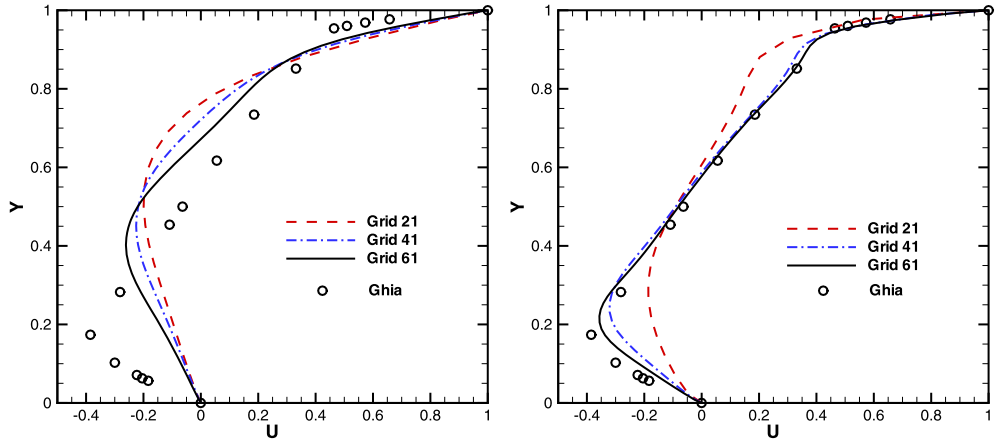

Fig. 9. The U velocity along the central line $x = 0.5$ on different meshes in the physical space (21×21, 41×41, 61×61). The left is from IMEX AP, and the right is from UGKS.

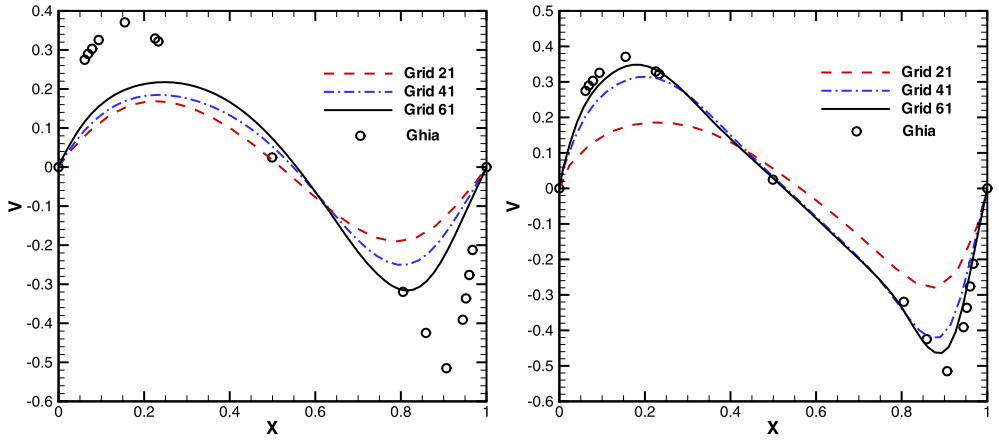

Fig. 10. The V velocity along the central line $y = 0.5$ on different meshes in the physical space (21×21, 41×41, 61×61). The left is from IMEX AP, and the right is from UGKS.

Then, we study the performance of UGKS+MBC and IMEX+KBC on coarse meshes. As shown in Figs. 9 and 10, the UGKS gets better velocity profiles on every mesh. Even on the 21×21 mesh, the UGKS with MBC still obtains two obvious eddies at the bottom corners, which is qualitatively correct.

These numerical results clearly show that the UGKS preserves AP property in the Navier–Stokes limit. We attribute such property to the analytical solution used in both flux solver and boundary condition of UGKS, because the analytical solution reflects the coupling of convection and collision. In continuum flow regime, these two processes are inseparable.

4. Dissipation from convection terms

The numerical experiments show that, although the implicit discretization of collision term guarantees the small deviation from the local equilibrium, the discretization of convection terms could still generate large artificial dissipation for the update of both conservative flow variables and the gas distribution function. As mentioned in Section 2.2, the distribution function f_i derived by Eq. (14) is a good approximation for NS limit. However, f_i is defined at cell center, which is updated through the interface flux $uf_{i+1/2}$. The interface flux controls the dissipative mechanism of the scheme. The difference between $f_{i+1/2}$ and its own equilibrium state $\mathcal{M}(f_{i+1/2})$ affects dissipation of the numerical scheme. Let's examine $f_{i+1/2}$ in these two AP schemes respectively.

4.1. IMEX flux without collision effect

The numerical flux of IMEX scheme is reformulated as,

$$\begin{aligned}\mathcal{F}_{IMEX} &= uf_{i+1/2} = u(H(u)f^l_{i+1/2} + (1-H(u))f^r_{i+1/2}) \\ &= u(g_{i+1/2} + [H(u)f^l_{i+1/2} + (1-H(u))f^r_{i+1/2} - g_{i+1/2}]).\end{aligned}$$

Here, $[H(u)f^l_{i+1/2} + (1-H(u))f^r_{i+1/2} - g_{i+1/2}]$ is an analogue of the Chapman–Enskog expansion. The corresponding viscous stress p_{11} is defined as below,

$$p_{11} = \int_{-\infty}^{+\infty} (u-U)(u-U)[H(u)f^l_{i+1/2} + (1-H(u))f^r_{i+1/2} - g_{i+1/2}]du.$$

Given $f_i = g_i + O(\tau)$, since the distribution functions $f^l_{i+1/2}$ and $f^r_{i+1/2}$ are interpolated from the distribution functions on their neighboring cells, the best estimations are as follows,

$$\begin{aligned}f^l_{i+1/2} &= g^l_{i+1/2} + O(\tau) = f^*_{i+1/2} + O(\Delta x^m), \quad m \geq 1, \\ f^r_{i+1/2} &= g^r_{i+1/2} + O(\tau) = f^*_{i+1/2} + O(\Delta x^m), \quad m \geq 1,\end{aligned} \tag{29}$$

where the superscript * denotes exact solution of a distribution function, and $O(\Delta x^m)$ denotes the truncation error. Substitute these formulas into p_{11}, then,

$$\begin{aligned}p_{11} &= \int_{-\infty}^{+\infty} (u-U)^2[H(u)g^l_{i+1/2} + (1-H(u))g^r_{i+1/2} - g_{i+1/2}]du + O(\tau), \\ &= D(\rho^l_{i+1/2}, U^l_{i+1/2}, T^l_{i+1/2}, \rho', U', T', O(\tau)),\end{aligned}$$

where $\rho' = \rho^r - \rho^l$, $U' = U^r - U^l$, $T' = T^r - T^l$ and D denotes a function. Obviously, when $\rho' = 0$, $U' = 0$, $T' = 0$, $O(\tau) = 0$, the distribution function $f_{i+1/2}$ is a Maxwell distribution, namely, $f_{i+1/2} = g_{i+1/2}$ and $p_{11} = 0$. In addition, $p_{11} \neq 0$ if one of ρ', U', T', $O(\tau)$ is nonzero. According to the Taylor expansion,

$$\begin{aligned}p_{11} &= D(\rho^l_{i+1/2}, U^l_{i+1/2}, T^l_{i+1/2}, 0, 0, 0, 0) + O(\rho') + O(U') + O(T') + O(\tau) \\ &= O(\rho') + O(U') + O(T') + O(\tau),\end{aligned}$$

when ρ', U', T', $O(\tau)$ approach to zero. This condition is fulfilled in Navier–Stokes shear flow, as the flow field is continuous. Then we use Eq. (29) to estimate ρ', U', T'.

$$\begin{aligned}< g^r_{i+1/2} - g^l_{i+1/2} > &= < f^*_{i+1/2} > - < f^*_{i+1/2} > + O(\Delta x^m) + O(\tau) \\ &= O(\Delta x^m) + O(\tau).\end{aligned}$$

Thus,

$$\begin{aligned}&\begin{pmatrix}\rho^r - \rho^l \\ \rho^r \mathbf{U}^r - \rho^l \mathbf{U}^l \\ \rho^r E^r - \rho^l E^l\end{pmatrix} = O(\Delta x^m) + O(\tau), \\ &\Rightarrow \rho' \sim U' \sim T' \sim O(\Delta x^m) + O(\tau),\end{aligned}$$

thereby, the viscous dissipation $p_{11} = O(\Delta x^m) + O(\tau)$.

As the van Leer limiter is first order accuracy at extreme point and second order accuracy in continuous region, the IMEX AP scheme with the van Leer slope limiter presents a dissipation proportional to Δx at extreme points and $(\Delta x)^2$ in other continuous region when the flow system approaches to the continuum limit.

4.2. UGKS flux with collision effect

The main difference between the IMEX AP and the UGKS is the construction of numerical flux. UGKS couples the collision and convection by a local analytical solution to evaluate flux. When Knudsen number approaches to zero, namely, $\Delta t/\tau \to \infty$, the numerical flux, formula (25), becomes,

$$\mathcal{F}_{UGKS} = u\{g_{i+1/2}[1-\tau(au+A)+\frac{1}{2}\Delta t A]+\frac{\tau}{\Delta t}[H(u)f^l_{i+1/2}+(1-H(u))f^r_{i+1/2}-g_{i+1/2}]+O(\tau^2)\}. \tag{30}$$

It is very close to Chapman–Enskog expansion. The first term of the UGKS flux is the Chapman–Enskog expansion with second order time accuracy [25]. The second term is almost identical with the non-equilibrium part in $\mathcal{F}_{IMEX}$. And this term is suppressed by a factor $\frac{\tau}{\Delta t}$. Using the estimation derived in the last subsection, the viscous dissipation for UGKS flux is $p_{11} = O(\tau\Delta x^m/\Delta t) + O(\tau)$. The dissipation of UGKS is much lower than the dissipation from IMEX AP since $\frac{\tau}{\Delta t} << 1$. Moreover, the leading term of UGKS dissipation is $O(\tau)$, which is consistent with NS limit. But for IMEX AP, the dissipation depends on the competition between $O(\tau)$ and $O(\Delta x^m)$. Therefore, IMEX AP only preserves Euler AP property, while UGKS could preserve NS AP property. In fact, in the continuum limit the collision term is so strong. No matter what kind of initial distribution function is, the distribution function approaches to the local equilibrium very rapidly during the whole convection stage. The formula (30), in which initial distribution function is suppressed by a factor $\frac{\tau}{\Delta t}$, demonstrates this property which is the most important key for NS AP schemes. Unfortunately, the simplest IMEX AP scheme fails to provide such a mechanism.

4.3. Coupling between convection and collision terms

The kinetic equation solver is always composed of a convection stage and a collision stage. The numerical flux is calculated on convection stage, and collision term is calculated on collision stage. Traditional numerical schemes always adopt operator splitting technique in order to simplify the numerical schemes. Only the convection term is considered on convection stage, while only collision term is considered on collision stage. The coupling between convection and collision is totally ignored within a time step and a cell size. The corresponding governing equation for each stage is,

$$\text{convection stage:} \quad f_t + \mathbf{u}\cdot\nabla f = 0,$$
$$\text{collision stage:} \quad f_t = \frac{g-f}{\tau}.$$

Bennoune et al. [13] proved that exactly solving the collision term without convection effect provides a distribution function too close to an equilibrium state, and cannot reproduce correct distribution function of the Navier–Stokes limit. In other words, the Chapman–Enskog expansion can be only achieved by including the convection term into the evaluation of the collision process. This can be easily understood because the convection term deviates the distribution function from the equilibrium and the collision drives it back to equilibrium. A NS distribution function needs proper balance between these two terms. In the past years, the importance of the coupling between convection and collision was first recognized in the evaluation of collision term [13–15,26]. So, the governing equations change into,

$$\text{convection stage:} \quad f_t + \mathbf{u}\cdot\nabla f = 0,$$
$$\text{collision stage:} \quad f_t + \mathbf{u}\cdot\nabla f = \frac{g-f}{\tau}.$$

In this paper, the numerical results and analysis have showed that the numerical flux calculated on convection stage still deviates from NS limit if the collision term is not included into the numerical flux. Thus, the coupling between convection and collision must be taken into account in the convective flux evaluation. The complete kinetic equation must be adopted for both convection stage and collision stage. That is,

$$\text{convection stage:} \quad f_t + \mathbf{u}\cdot\nabla f = \frac{g-f}{\tau},$$
$$\text{collision stage:} \quad f_t + \mathbf{u}\cdot\nabla f = \frac{g-f}{\tau}.$$

Due to the major contribution of particle collision in the near continuum flow regime, it is crucial to evaluate the collision term in the convective flux evaluation. UGKS provides a promising methodology which utilizes local analytical solution of kinetic equation to construct numerical flux.

On macroscopic level, convection and collision effect are tightly coupled with each other. Any absence of collision or convection will not deduce the Chapman–Enskog NS expansion, and make the numerical results departure from the Navier–Stokes limit.

5. Criteria for Navier–Stokes limit asymptotic preserving scheme

As implied by the Chapman–Enskog expansion, in order to recover the Navier–Stokes limit, the schemes have to be capable of capturing the term on the order $O(\tau)$. In the past decades, many numerical schemes concentrate on the precise prediction of collision terms, thereby the numerical treatment of convection term is left behind. According to the analysis and numerical results in this study, we propose three criteria for the NS AP schemes. To recover the Navier–Stokes limit, an AP scheme should preserve the following criteria,

- the numerical scheme is stable regardless of τ,
- the numerical flux is mainly determined from the emerging equilibrium state due to intensive particle collisions, instead of the initially reconstructed gas distribution function,
- the numerical flux is consistent with the Chapman–Enskog NS expansion.

Note that the numerical flux is emphasized, rather than the distribution function itself. With the same spirit, the UGKS framework has been successfully extended to the diffusion limit of linear kinetic models [23].

6. Conclusion

This paper investigates the performance of two standard AP schemes in the Navier–Stokes limit. The 2D lid-driven cavity flow is used as a benchmark test case, and is simulated by UGKS and IMEX AP scheme respectively. The numerical results and analysis demonstrate that the UGKS could capture the Navier–Stokes limit more accurately. The coupling between the convection and collision is essentially important for the Navier–Stokes limit. The implementation of local analytical solution can reproduce such a coupling during a whole gas evolution process within a time step. The UGKS provides a general framework to construct numerical schemes in all flow regimes, because most kinetic equations have relaxation terms which can be explicitly solved along the characteristic lines. The setup of the benchmark test case in this paper is also important for the whole AP society, because significant amount of newly developed AP schemes have never been seriously tested in two dimensional cases.

Acknowledgements

This work was supported by Hong Kong Research Grant Council (621011, 620813, 16211014), and grants SBI14SC11 and IRS15SC29 at HKUST.

References

[1] S. Chapman, T.G. Cowling, The Mathematical Theory of Non-Uniform Gases, Cambridge University Press, 1970.
[2] P. Degond, S. Jin, L. Mieussens, A smooth transition model between kinetic and hydrodynamic equations, J. Comput. Phys. 209 (2005) 665–694.
[3] V. Kolobov, R. Arslanbekov, V. Aristov, A. Frolova, S. Zabelok, Unified solver for rarefied and continuum flows with adaptive mesh and algorithm refinement, J. Comput. Phys. 223 (2007) 589–608.
[4] S. Tiwari, A. Klar, An adaptive domain decomposition procedure for Boltzmann and Euler equations, J. Comput. Appl. Math. 90 (1998) 223–237.
[5] S. Jin, Asymptotic preserving (AP) schemes for multiscale kinetic and hyperbolic equations: a review, in: Lecture Notes for Summer School on "Methods and Models of Kinetic Theory" (M&MKT), Porto Ercole, Grosseto, Italy, 2010, Riv. Mat. Univ. Parma 3 (2012) 177–216.
[6] R.E. Caflisch, S. Jin, G. Russo, Uniformly accurate schemes for hyperbolic systems with relaxation, SIAM J. Numer. Anal. 34 (1997) 246–281.
[7] E. Gabetta, L. Pareschi, G. Toscani, Relaxation schemes for nonlinear kinetic equations, SIAM J. Numer. Anal. 34 (1997) 2168–2194.
[8] S. Jin, C.D. Levermore, Numerical schemes for hyperbolic conservation laws with stiff relaxation terms, J. Comput. Phys. 126 (1996) 449–467.
[9] S. Jin, Runge–Kutta methods for hyperbolic conservation laws with stiff relaxation terms, J. Comput. Phys. 122 (1995) 51–67.
[10] K. Xu, Numerical hydrodynamics from gas-kinetic theory, Ph.D. thesis, Columbia University, 1993.
[11] K. Xu, A gas-kinetic BGK scheme for the Navier–Stokes equations and its connection with artificial dissipation and Godunov method, J. Comput. Phys. 171 (2001) 289–335.
[12] K. Xu, J. Huang, A unified gas-kinetic scheme for continuum and rarefied flows, J. Comput. Phys. 229 (2010) 7747–7764.
[13] M. Bennoune, M. Lemou, L. Mieussens, Uniformly stable numerical schemes for the Boltzmann equation preserving the compressible Navier–Stokes asymptotics, J. Comput. Phys. 227 (2008) 3781–3803.
[14] F. Filbet, S. Jin, A class of asymptotic-preserving schemes for kinetic equations and related problems with stiff sources, J. Comput. Phys. 229 (2010) 7625–7648.
[15] F. Filbet, S. Jin, An asymptotic preserving scheme for the ES-BGK model of the Boltzmann equation, J. Sci. Comput. 46 (2011) 204–224.
[16] A. Klar, An asymptotic preserving numerical scheme for kinetic equations in the low Mach number limit, SIAM J. Numer. Anal. 36 (1999) 1507–1527.
[17] U. Ghia, K. Ghia, C. Shin, High-Re solutions for incompressible flow using the Navier–Stokes equations and a multigrid method, J. Comput. Phys. 48 (1982) 387–411.
[18] P.L. Bhatnagar, E.P. Gross, M. Krook, A model for collision processes in gases, Phys. Rev. 94 (1954) 511.
[19] S. Pieraccini, G. Puppo, Implicit–explicit schemes for BGK kinetic equations, J. Sci. Comput. 32 (2007) 1–28.
[20] K. Xu, J. Huang, An improved unified gas-kinetic scheme and the study of shock structures, IMA J. Appl. Math. 76 (2011) 698–711.
[21] J. Huang, K. Xu, P. Yu, A unified gas-kinetic scheme for continuum and rarefied flows II: multi-dimensional cases, Commun. Comput. Phys. 12 (2012) 662–690.
[22] J. Huang, K. Xu, P. Yu, A unified gas-kinetic scheme for continuum and rarefied flows III: microflow simulations, Commun. Comput. Phys. 14 (2013) 1147–1173.
[23] L. Mieussens, On the asymptotic preserving property of the unified gas kinetic scheme for the diffusion limit of linear kinetic models, J. Comput. Phys. 253 (2013) 138–156.

[24] G.A. Bird, Molecular Gas Dynamics and the Direct Simulation of Gas Flows, Clarendon Press, Oxford, 1994.
[25] T. Ohwada, S. Kobayashi, Management of discontinuous reconstruction in kinetic schemes, J. Comput. Phys. 197 (2004) 116–138.
[26] Q. Li, L. Pareschi, Exponential Runge–Kutta schemes for inhomogeneous Boltzmann equations with high order of accuracy, J. Comput. Phys. 259 (2014) 402–420.